Journal of Archaeological Science 40 (2013) 1703–1714

Contents lists available at SciVerse ScienceDirect

Journal of Archaeological Science

journal homepage: http://www.elsevier.com/locate/jas

Archaeomagnetic data from three Punic sites in Tunisia

Boutheina Fouzai [a], Lluís Casas [b,*], Nejia Laridhi Ouazaa [a], Mounir Fantar [c], Aureli Álvarez [b]

[a] Université de Tunis El Manar, Faculté des Sciences, Département de Géologie, Campus Universitaire, 2092 Manar II, Tunisia
[b] Universitat Autònoma de Barcelona, Facultat de Ciències, Departament de Geologia, Campus de la UAB, 08193 Bellaterra, Catalonia, Spain
[c] Institut National du Patrimoine, 4, Place du Château Bab Menara, 1008 Tunis, Tunisia

ARTICLE INFO

Article history:
Received 10 August 2012
Received in revised form
19 November 2012
Accepted 2 December 2012

Keywords:
Archaeomagnetism
Dating
Geomagnetic field modeling
Tunisia
Archaeodirection
Archaeointensity
Punic civilization

ABSTRACT

Archaeomagnetic analyses on bricks and slag fragments from kilns have been undertaken. Four new archaeomagnetic directions and two new archaeomagnetic intensities have been reported for three Punic sites in Tunisia. The SCHA.DIF.3K archaeomagnetic model gives the most consistent age estimates, in agreement with the archaeological ages for three of the four analyzed kilns. The archaeomagnetic models appeared to be surprisingly proficient both using archaeodirections and intensities for El Maklouba. The existence of kilns from different chronological archaeological phases (4th–3th century BC and 2nd–3rd century AD) has been confirmed for this site. The archaeological hypothesis that associates the kiln in El Gaala with the neighboring Punic necropolis is compatible with the archaeomagnetic data obtained from the kiln, though a modern use or remagnetisation of the kiln cannot be excluded.

1. Introduction

Archaeomagnetic data can be retrieved from archaeological materials that were burnt or baked in the past. When any archaeological material containing magnetic grains is heated above their magnetic transition temperatures it loses any previous remanent magnetization and as it cools down acquires a thermoremanent magnetization (TRM) that relates to the prevailing geomagnetic field, the TRM can be kept stored in the material unless it is reheated or chemically altered. If the archaeological age of the materials is well known, these stored data can be used to produce regional or global archaeomagnetic field models that describe the time and space evolution of the geomagnetic field. Accurate models can be used as dating tools, though the accuracy of the models rely on the availability and quality of experimental data near the area under study (Casas et al., 2008). The development of archaeomagnetism-related research is just starting in the northern Africa area. Until recently, only very few data were available in this area (Casas et al., 2008; Kovacheva, 1984; Najid, 1986; Thellier and Thellier, 1959). New data has been published for Tunisia (Fouzai et al., 2012; Gómez-Paccard et al., 2012). These recent research, along with the one presented here, should contribute to a better knowledge of the local behavior of the geomagnetic field and therefore to develop accurate archaeomagnetic dating tools for Tunisia. Tunisia has a rich cultural heritage covering a wide historical time range, previously published data deal with Roman (Fouzai et al., 2012) and Medieval (Gómez-Paccard et al., 2012) times. We focus here on the Punic era, we have applied archaeomagnetic techniques on kilns from three Punic sites of Tunisia: El Maklouba and El Gaala (Sahel region) and Kerkuane (Cap Bon) (see Fig. 1).

2. Historical and archaeological background of the studied sites

2.1. El Maklouba

The site of El Maklouba consists of a broad mound 2 km to the north of Ksour Essef (42 km south from Monastir) in the Sahel region. Peacock et al. (1989) reports the features of the site and the product of its own prospections undertaken in 1985: the mound is a tell formed by the remains of what probably was a small town with an industrial zone along the south western edge. This edge was excavated during the sixties (20th century) and it was left partially open. Among the features of the site, there are the remains of 12 kilns of various sizes, cisterns and building walls. The 1985 prospection produced, among other materials, fragments of

* Corresponding author. Tel.: +34 935868365; fax: +34 935811263.
E-mail address: Lluis.Casas@uab.cat (L. Casas).

0305-4403/$ – see front matter © 2012 Elsevier Ltd. All rights reserved.
http://dx.doi.org/10.1016/j.jas.2012.12.004

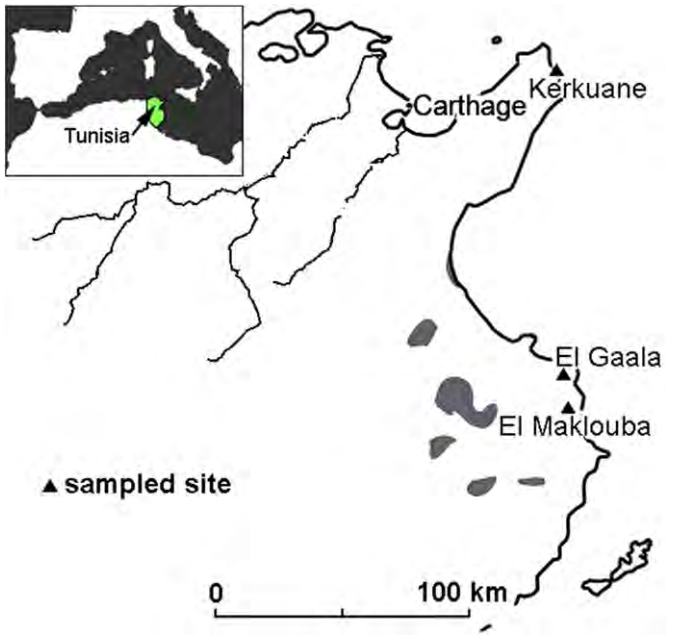

Fig. 1. Location of the sampled archaeological sites in Tunisia.

production waste amphorae. The majority of amphorae rims were identified as Punic: various Maña and van der Werffs forms that date between the first half of the 2nd century BC and the 1st century AD, but also earlier forms (Maña D). According to Gibbins (2001), the earliest forms permit to categorize the site as the earliest kiln complex in central Tunisia with amphorae being manufactured from the 4th century BC, although the main period of activity would be in the 2nd and 1st centuries BC (Pasa, 2011). Later amphorae fragments were also identified (Africana 1A), this would indicate either small-scale production in the late 2nd or 3rd centuries AD with or without continuity of production from the previous centuries (Peacock et al., 1989). Productions from this site have been identified among the cargoes of Roman shipwrecks (Taylor et al., 1997).

2.2. El Gaala

El Gaala is a little known archaeological site, located about 4 km north-west from ancient Thapsus, near the modern town of Teboulba. The site was excavated in 1995 (Ben Younés, 2002). Much of the remains from the site have disappeared due to modern quarrying works in the area. Despite the damage, the site comprises a conical pottery kiln dug into the hill (only the combustion chamber is preserved), a necropolis also dug into the hill (disappeared to a great extend) and traces of pre-Roman quarrying works. Lamps retrieved from the only intact shaft tomb indicate that the necropolis was in use from the mid-4th century BC to the 1st century BC. Later remains include a Christian basilica from the 6th–7th century AD (Ben Lazreg and Duval, 1995). Ben Younés, 2002 speculates over the possible link between the necropolis and the kiln. According to him, the necropolis could have served a community of potters, and possibly the preserved kiln would not be the only one in the area.

2.3. Kerkuane

Kerkuane is a renowned Punic site, declared in 1985 a World Heritage Site by Unesco, that welcomes visitors to its ruins and museum. It is located on a cliff that dominates the sea, in the northern end of the Cap Bon, 12 km north of Kélibia. The site was fortuitous discovered by two French archaeologists and soon afterwards the first excavations were undertaken (during the fifties of the 20th century). The site consists of several necropolises and a double walled town. The graves cover a long period, from the 6th to 3rd century BC (Fantar, 1984). The oldest ceramic datable fragments are Greek B2 Ionian cups that date back from 6th century BC (Morel, 1969), though the urban fabric is basically from the late-4th century BC to the early-3rd century BC (Fantar, 2000). From the imported datable material found in the last occupation level of the site, it has been deduced that the city was presumably abandoned in the mid-3rd century BC (Morel, 1969) after being destroyed by the Romans during the First Punic War. The exceptionality of the site is that, contrary to other Punic cities, the town was not reoccupied and therefore its Punic features have been preserved intact (Fantar, 1984). There are both pottery and lime kilns in the site, the first are found outside and inside the city walls whereas the second are always outside the inner walls and sometimes the outer walls rise over them (Fantar, 1986). Kerkuane is one of the few Punic sites with attested lime kilns.

3. Materials sampled

Six identified kilns were sampled in the three studied sites. Several oriented cylindrical samples (~2.5 cm diameter) were collected from them using a portable electrical drill with a water-cooled diamond bit, following the standard palaeomagnetic sampling procedure. The in-situ azimuth and dip of the cores were measured using a compass coupled to a core orienting fixture. In case of breaking the cylinder before taking its orientation, if possible, the cylinder was carefully put back in place in its hole to mark its orientation. The samples were taken from parts of the kilns with clear evidence of repeated exposure to intense heat during firing; when possible, structures covered by melting products (slag) were sampled. The samples taken were not very long in order to collect parts that were closer to the heat source; in general each sample produced a single specimen.

Two pottery kilns (M1 and M2) were sampled in El Maklouba (Fig. 2). Both were not totally excavated and M2 was actually almost invisible. However, the upper parts of their remains were accessible to collect samples in situ. Given that the archaeological value of the remains is moderate, we were allowed to sample intensively the accessible remains. Thus, we also collected non-oriented brick and slag fragments, from both kilns and slag fragments from unidentified kilns (labeled simply as M samples). These were cut into standard cylindrical specimens in the laboratory, the spare material was crushed and kept to perform magnetic mineralogy analyses.

The El Gaala kiln (G1) has an inverted truncated-cone shape and is cut into the hill, its preserved depth amounts 3.8 m, its upper part consists of a double-thickness cylindrical wall of stone bricks in the outer part and mud-bricks in the interior, the inner wall was possibly built at a later stage to repair the kiln (Ben Younés, 2002). Mainly, the inner part of the outer wall was sampled to retrieve oriented samples (Fig. 3). The inner wall was very crumbly and only two samples were retrieved from it.

Three kilns (K1, K2 and K3) were sampled in Kerkuane. Sampling was limited to few drills in order to preserve the visitable structures. Kiln K1 is one of the first features that the guest finds when follows the touristic path of the site, it is a small pottery kiln located outside the city walls before the construction of the second outer wall (Fig. 4). It is fully excavated, the preserved remains include the first brick layers, which highlight the outline of the cylindrical chamber and a passageway, and a central pillar made of a pile of circular bricks. We limited sampling on this kiln to only two oriented cores from the central pillar in order to avoid undue

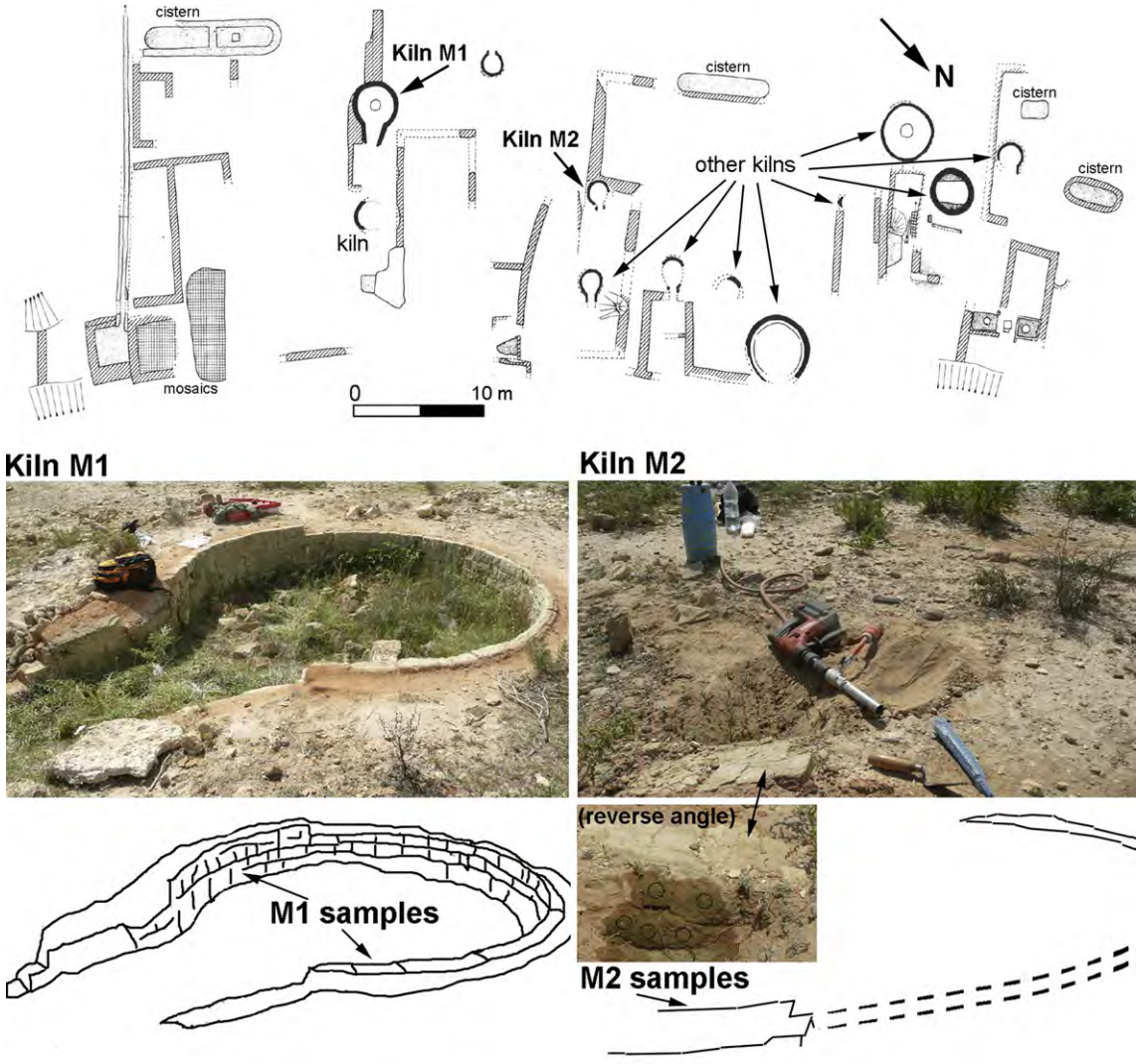

Fig. 2. Plan of the previously excavated area in El Maklouba, adapted from Peacock et al. (1989), sampled kilns M1 and M2 are identified on it (top). Photographs and sketches of the sampled kilns (bottom).

damage. Kiln K2 is a bigger and much more damaged pottery kiln, it locates near the southern gate (Fig. 4); four oriented samples were retrieved from it. Finally, two more oriented cores were drilled in kiln K3, which is one of the circular lime kilns of the site. It is also quite damaged; it locates near the coastal cliff (Fig. 4) and corresponds to the described *Four V* in Fantar (1986). Extracted cores were resent to the site person in charge to be replaced in its original holes after reading its magnetic data.

To sum up, 65 specimens were obtained from three archeological sites from Tunisia with presumed ages ranging from the 4th century BC to the 3rd century AD. Table 1 summarizes the details of all the sites and samples.

4. Experimental methods and data analyses

The archaeomagnetic vector was studied using the facilities available at the paleomagnetic laboratory of Barcelona (SCT UB-CSIC). Directional measurements were applied to oriented samples from all the studied sites following the equipment and methods described in Fouzai et al. (2012) and applying the same procedure to represent the obtained data and the same selection criteria. When more than one specimen was available from an independently oriented sample, the most reliable demagnetization experiment, in terms of maximum angular deviation (Kirschvink, 1980) was always retained. Computation of mean directions for each structure or site was achieved by using Fisher (1953) statistics; concentration parameter k and confidence factor α_{95} were also obtained.

Archaeointensity measurements were carried out on the non-oriented samples from El Maklouba. Their magnetic mineralogy was investigated using magnetic susceptibility equipment from Bartington, available at the Geology Department in the Universitat Autònoma, in Barcelona (UAB), consisting of an MS3 magnetic susceptibility meter and two kinds of sensors (MS2B dual frequency and MS2W water jacketed). Mössbauer spectra were also recorded at room temperature on several powdered samples using a transmission Mössbauer spectrometer with a ^{57}Co/Rh source from the Material Science Institute in Barcelona (ICMAB-CSIC). Archaeointensity was determined using the Coe variant method of a Thellier-type experiment (Coe, 1967) with several alteration and reversibility tests as described in Fouzai et al. (2012). The external field for the required applied field steps was 50 μT. Taking into account that our samples consist of slag fragments or bricks covered by melting products, we considered that the TRM

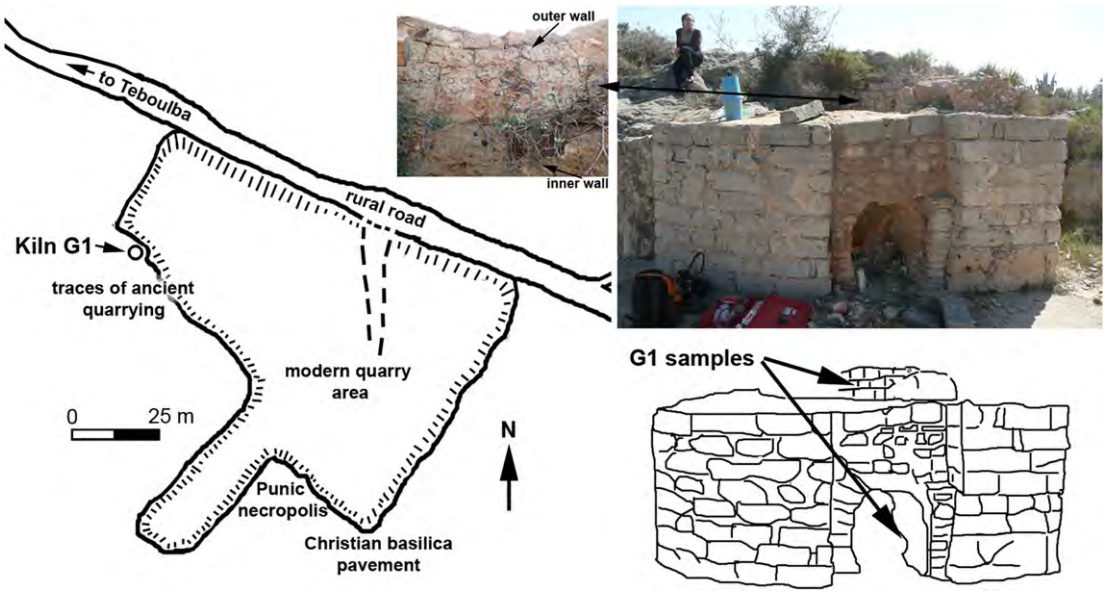

Fig. 3. Plan of the existing features in El Gaala, sampled kiln G1 is identified on it (left). Photograph and sketch of the sampled kiln (right). Inset on the left is a photograph of the kiln wall from the interior, inner and outer walls are clearly seen.

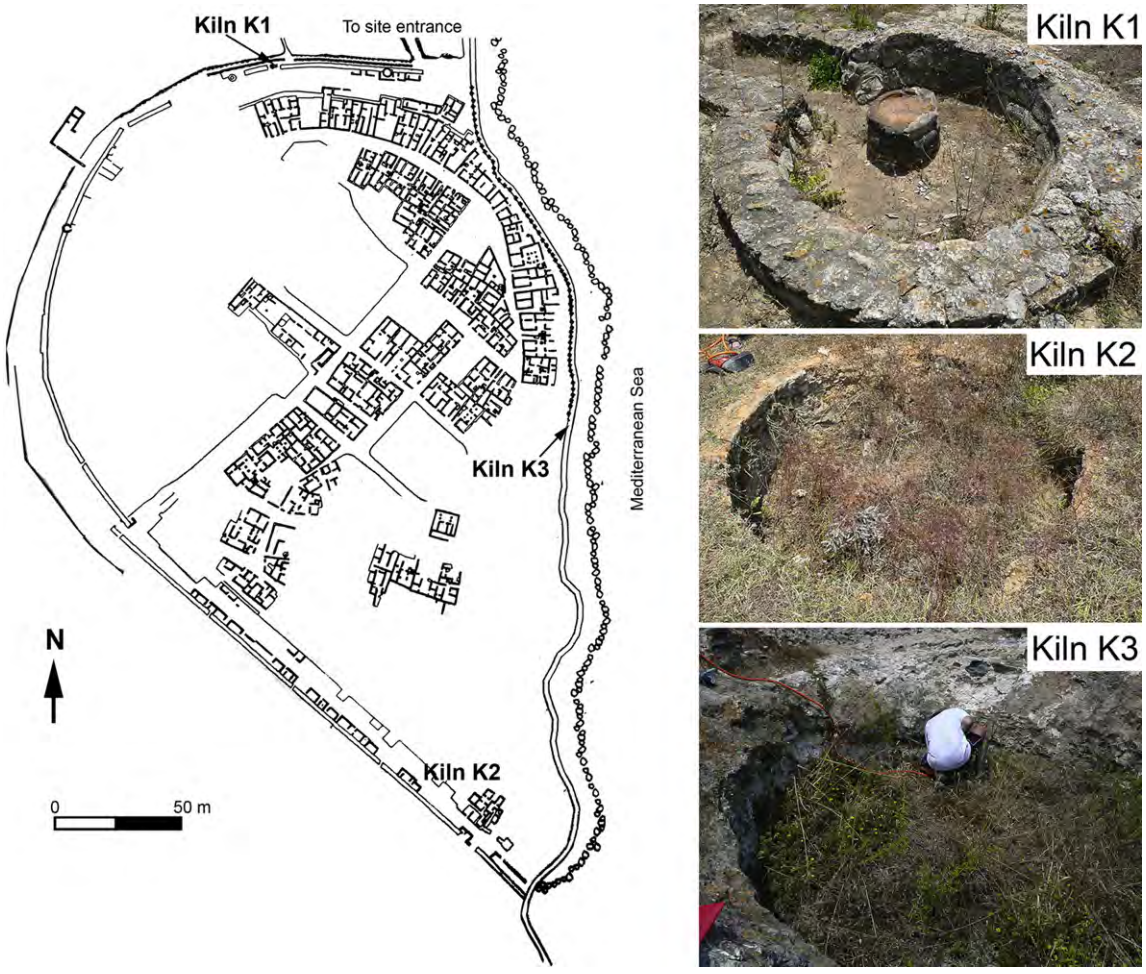

Fig. 4. Plan of the archaeological site of Kerkuane, sampled kilns K1, K2 and K3 are identified on it (left). Photographs of the sampled kilns (right).

Table 1
Coordinates of the sampled sites (Lat., latitude and Long., longitude) with indication of their presumed ages according to archaeological evidence, sample labels and number of collected samples; n is the number of standard specimens obtained from the N collected samples; n_u is the number of specimens used to compute archaeomagnetic directions or intensities.

Site	Lat. (°N)	Long. (°E)	Presumed age	Label	Purpose	n/N	n_u
El Maklouba	35.26	11.00	4th BC–3rd AD	M1	Direction	11/10	8
				M1	Intensity	7/7	7
				M2	Direction	8/8	8
				M2	Intensity	7/7	4
				M[a]	Intensity	2/2	–
El Gaala	35.38	11.00	4th–1st BC	G1	Direction	21/18	12
Kerkuane	36.57	11.06	4th–3rd BC	K1	Direction	2/2	2
				K2	Direction	4/4	2
				K3	Direction	3/2	3

[a] Brick and slag from unidentified kiln/s.

anisotropy effect upon archaeointensity estimates can be taken as insignificant. For instance, Kovacheva et al. (2009) found that the anisotropy correction of intensity results for materials other than pottery seems negligible and thus no correction of this effect has been performed. In contrast, we performed a cooling rate test following the procedure described in Chauvin et al. (2000), the test was performed at 560 °C with a quick cooling (~95 min) for the first and third heating (TRM_1 and TRM_3) and a slow cooling (~12 h) for the second heating (TRM_2). The effect of the cooling rate upon the magnetization was calculated as the ratio: $r_1 = (TRM_2 - TRM_1)/TRM_1$ and the changes in the TRM acquisition capacity as the ratio: $r_2 = (TRM_1 - TRM_3)/TRM_1$. Cooling rate correction was applied only when the corresponding r_2 was <5%. For each structure every sample-datum was plotted as a Gaussian function and, to compute an overall archaeointensity value, a Gaussian function was fitted to the sum of all individual results.

The results were compared with model predictions using a Matlab dating tool developed by Pavón-Carrasco et al. (2011). Three models were used: the regional model SCHA.DIF.3K (Pavón-Carrasco et al., 2009) and the global models CALS3K.3 (Korte et al., 2009) and CALS3K.4b (Korte and Constable, 2011). The SCHA.DIF.3K model was obtained by least-sums of absolute deviation inversion of paleomagnetic data using spherical cap harmonics (SCHA) and provides geomagnetic field vector values over the European continent, northern Africa and western Asia from 1000 BC to 1900 AD. The CALS3K.3 model was generated using a compilation of archaeomagnetic and lake sediments data covering the past 3000 years. Although CALS3K.3 is a global model, the distribution of data is strongly biased towards the northern hemisphere, and Europe in particular, thus the model provides reasonable field values especially for this area. CALS3K.4b model is the last available update of CALS3K models where data additions, mainly from south-east Asian, Alaskan and Siberian regions, have been done. Also, uncertainties estimates from bootstrap experiments have been included. The use of archaeomagnetic field models avoids the

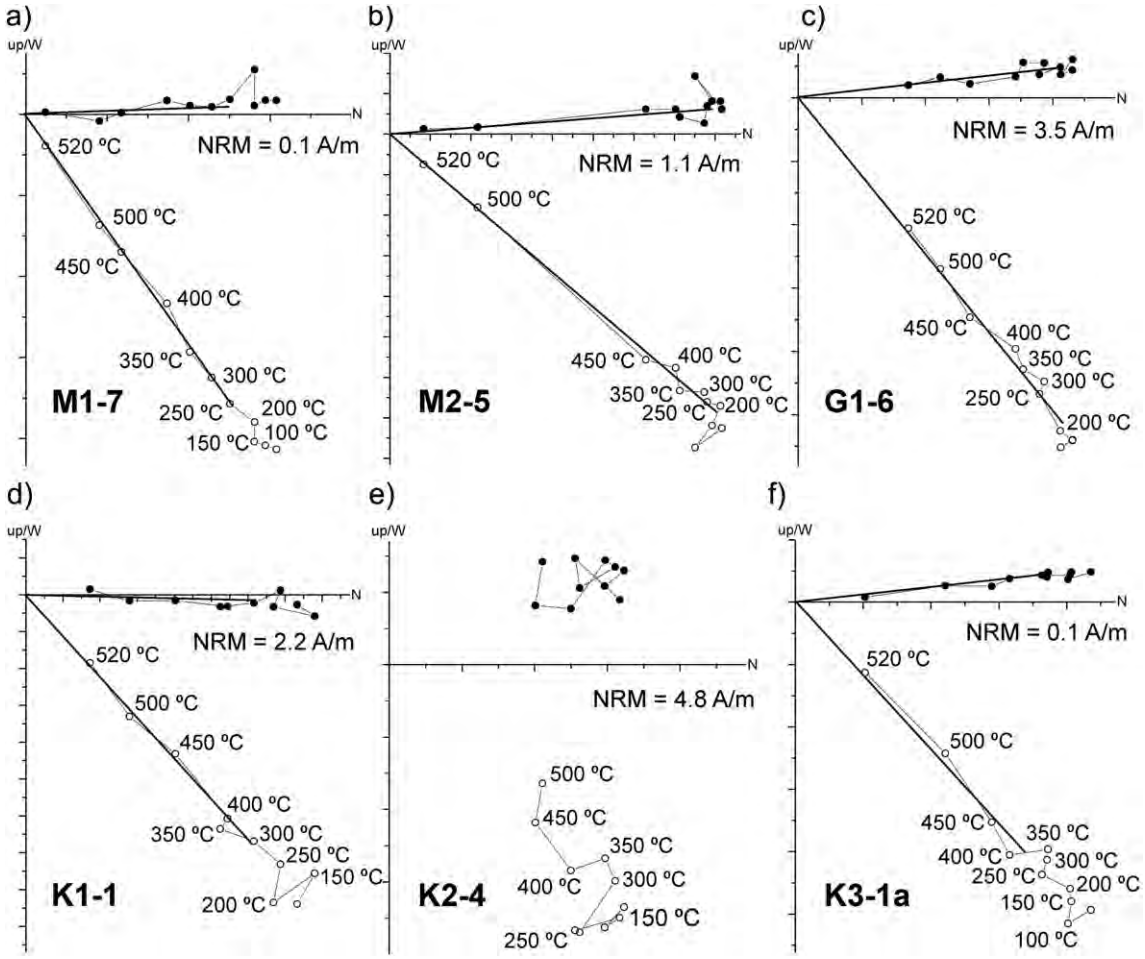

Fig. 5. Representative Zijderveld plots depicting the orthogonal projection of the remanent magnetization vectors during progressive demagnetization for different specimens from El Maklouba, El Gaala and Kerkuane. Open (solid) symbols represent projections on vertical (horizontal) planes. Lines indicate the ChRM directions.

need for relocation of archaeomagnetic data to a central location, which is a procedure that involves inherently an error (Casas and Incoronato, 2007).

5. Results and discussion

5.1. Archaeodirectional results and discussion

Representative Zijderveld diagrams of specimens from El Maklouba, El Gaala and Kerkuane are shown in Fig. 5. A total of 49 specimens were analyzed. Three specimens from M1 were rejected, two of them due to inconsistent archaeomagnetic directions attributable to a wrong replacement of a broken core and another one due to MAD >5. Seven specimens from G1 were rejected, again due to the break of the core during sampling (two specimens) and MAD >5 (two specimens); two more specimens were rejected because the maximum applied temperature (520 °C) hardly demagnetized a very small percentage of the NRM though the measured direction was consistent with ChRM directions obtained for the rest of G1 specimens. NRM direction measured on specimens from the pottery kilns from Kerkuane (K1 and K2) showed a quite erratic behavior, with the sole exception of K1-1 specimen (Fig. 5d). ChRM direction was often defined only after considerable demagnetization, and in two cases demagnetization was not achieved at all (Fig. 5e), these two specimens had to be rejected. In contrast, archaeomagnetic directions measured on specimens from the lime kiln (K3) were far sharper, but unfortunately only two cores (three specimens) were available from it.

Fig. 6 shows the stereographic projection of the non-rejected archaeomagnetic directions calculated for each sample. Results from El Maklouba (Fig. 6a) indicate that archaeomagnetic directions stored in the two analyzed kilns (M1 and M2) are distinctly different. A single archaeomagnetic mean direction has been obtained for El Gaala (Fig. 6b), the two samples taken from the inner wall lie a bit far from the mean direction (open dots in Fig. 6) and were finally removed from the calculation of the mean to avoid mixing data from two possibly different kiln heatings that are separated by an undefined gap of time. The three sampled kilns in Kerkuane have a similar archaeological setting as all of them are located on or outside the inner walls of the city. This fact, together with the low number of samples from each kiln and the homogeneity of the obtained archaeodirections has driven us to compute a single mean value for the three sampled kilns of this site. It is worth to note that despite the relatively high quality of the mean archaeodirection for Kerkuane, its estimation is based on only six values. The ensemble of obtained archaeomagnetic directional results is summarized in Table 2.

Comparing the results with the SCHA.DIF.3K model we obtained probability density functions of possible dates for both declination and inclination. The intersection of these functions produces the most probable dates (see Figs. 7 and 8). The two kilns sampled at El Maklouba produce different results. For the M1 kiln (Fig. 7a), the combined probability function indicates basically two solutions (BC 417–17 or AD 1687–1852). The first solution is in agreement with the main period of activity in the site as indicated by archaeological evidence, the second solution would indicate a heating of the structure out of his archaeological context and would imply that it was exposed uncovered during that period. For the M2 kiln (Fig. 7b), the SCHA.DIF.3K model points to a single solution (AD 118–425), consistent with the progression of activity during the Roman times, as indicated by the presence of Africana 1A fragments on the site (Peacock et al., 1989). The obtained solution for the kiln sampled at El Gaala (Fig. 8a) distributes basically in a 19th–20th century AD peak and in three probability peaks within the BC 68–AD 483 time interval with a distinct main peak pointing to year

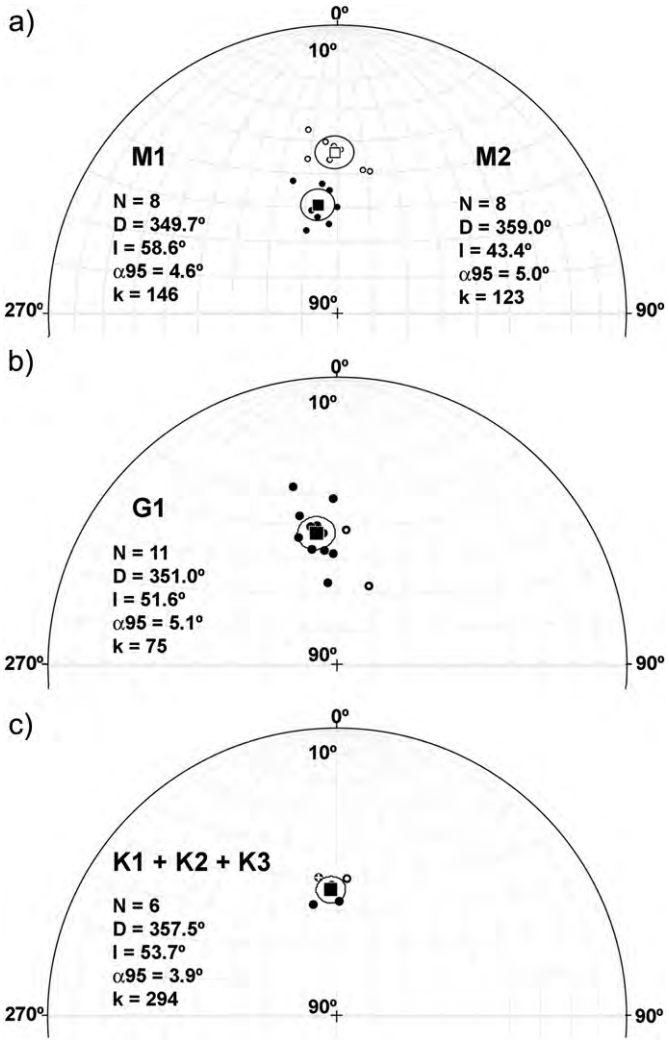

Fig. 6. Stereographic projection of the archaeomagnetic directions calculated for each sample from (a) El Maklouba, solid (open) symbols belong to kiln M1 (M2); (b) El Gaala, open symbols correspond to samples from the inner wall; (c) Kerkuane, solid (open/crossed) circle symbols correspond to K1 (K2/K3) kilns. Mean directions and α_{95} error circles for kilns M1, M2, G1 and the three kilns from Kerkuane (K1, K2 and K3) merged together are shown. *N* indicates the number of independently oriented sample taken into account for the calculation of the mean; *D* and *I* stands for declination and inclination; α_{95} and *k*, 95% confidence cone of mean directions and precision parameter from Fisher statistics.

24 BC, which matches well with the last use of tombs in the nearby necropolis, and thus the result is compatible with the presumed contemporaneity between the kiln and the necropolis (Ben Younés, 2002). However, a significant part of the probability (the 19th–20th century AD peak) would suggest a recent remagnetization of the

Table 2
Archaeomagnetic directional results.

Name	Lat (°N)	Long (°E)	*N*	D (°)	I (°)	*k*	α_{95} (°)
El Maklouba (M1)	35.26	11.00	8	349.7	58.6	146	4.6
El Maklouba (M2)	35.26	11.00	8	359.0	43.4	123	5.0
El Gaala (G1)	35.38	11.00	11	351.0	51.6	75	5.1
Kerkuane (merged)	36.57	11.06	6	357.5	53.7	294	3.9

Columns from left to right: name, name of the site (structure); Lat. and Long., Latitude and Longitude of the site; *N*, number of samples taken into account in the calculation of the mean site direction; D, archaeomagnetic declination; I, archaeomagnetic inclination; *k* and α_{95}, precision parameter and 95% confidence limit of characteristic remanent magnetization, from Fisher statistics.

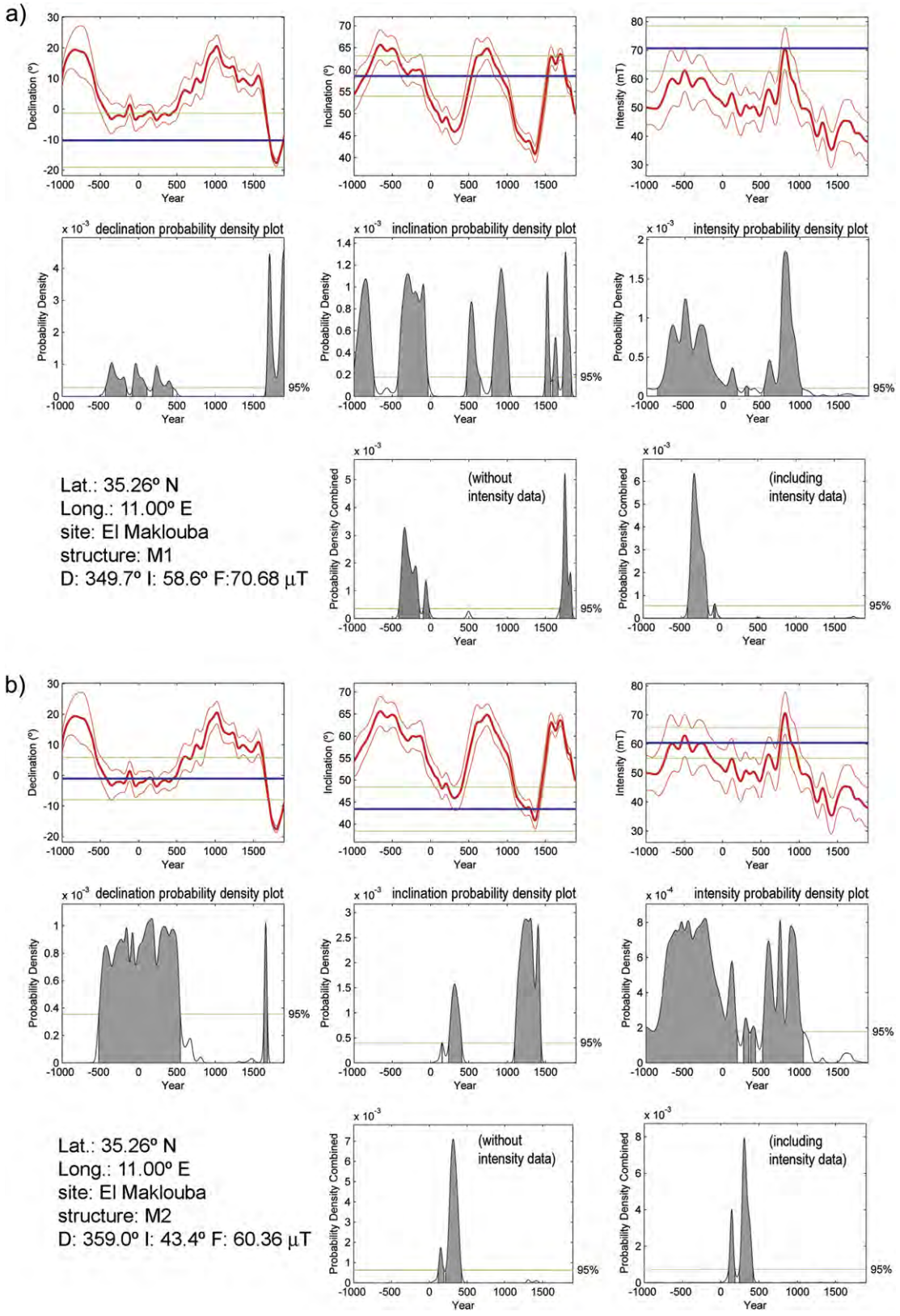

Fig. 7. Probability-of-age density functions obtained with the Matlab tool from Pavón-Carrasco et al. (2011) for El Maklouba kilns (a) M1 and (b) M2, using SCHA.DIF.3K model. On the bottom: location of the sites, experimental mean directions and intensities and both combined (declination and inclination) and combined (declination, inclination and intensity) probability functions.

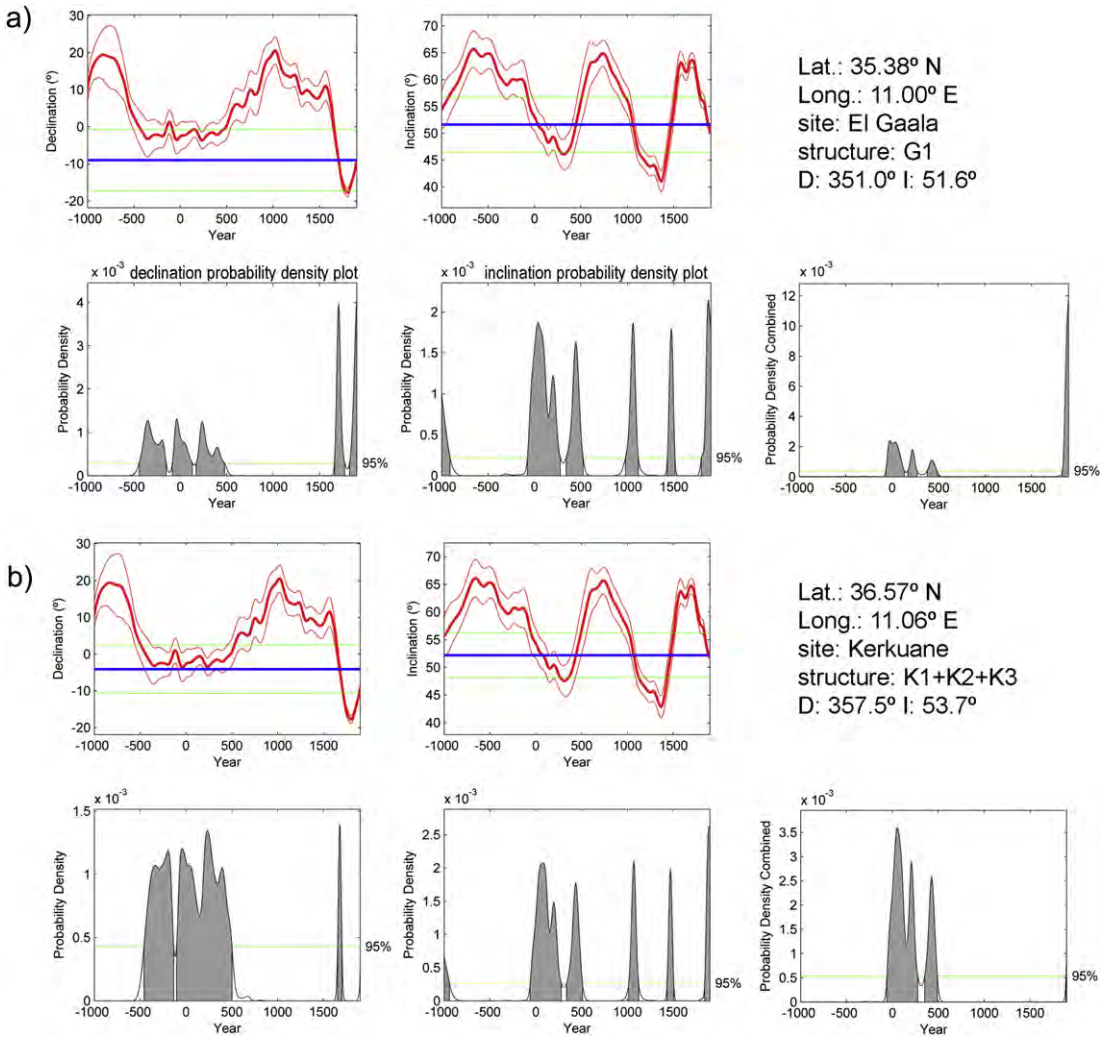

Fig. 8. Probability-of-age density functions obtained with the Matlab tool from Pavón-Carrasco et al. (2011) for (a) G1 kiln from El Gaala and (b) K1, K2 and K3 kilns from Kerkuane, using SCHA.DIF.3K model. On the right: location of the sites, experimental mean directions and combined (declination and inclination) probability functions.

kiln. The mean archaeodirection for Kerkuane is based on only 6 values and even from 3 different structures. Although the 6 values group very well, the statistical value could be meaningless and thus the results must be considered preliminary. The results indicate that the last firing of the kilns or its remains would have happened within the first 5 centuries AD, and thus the archaeomagnetic does not agree at all with the likely archaeological age that points toward an abandonment of the city in the mid-3rd century BC (Morel, 1969).

Apparently, the solutions yielded by the SCHA.DIF.3K model are compatible with the archaeological evidence with the sole exception of Kerkuane, although we note that the number of investigated samples is too low to consider that the result has statistical meaning. Using global models the results are less promising. Both CALS3K.3 and CALS3K.4b produced probability distributions broader than those using SCHA.DIF.3K (see Fig. 9 and Table 3). The CALS3K distributions cover the presumed archaeological time intervals but spread far outside them, covering most of the 3000 years within which the models apply. Particularly, CALS3K.3 exhibits complicated multipeak structures whereas the bootstrap averaged CALS3K.4b model shows highly smoothed profiles (except for the period middle 19th century onwards). Some tests were also performed using the higher resolution CALS3K.4 model (Korte and Constable, 2011), but as uncertainties are not provided with this model, the Matlab dating tool produced unnecessarily spiky distributions though, in essence, similar to those from CALS3K.3 model.

5.2. Magnetic mineralogy and archaeointensity results from El Maklouba

Archaeomagnetic dating of El Maklouba has been refined performing archaeointensity analysis for this site. However, this analysis requires a particular magnetic mineralogy: thermal alteration, multidomain grains and interactions among grains have to be absolutely avoided (Carvallo et al., 2006). In order to better understand the behavior of the specimens in the archaeointensity experiments and to check their thermal stability, magnetic susceptibility and Mössbauer measurements were performed on powdered sister samples of the cylindrical cores. From room temperature magnetic susceptibility measurements, performed at two different frequencies (470 and 4700 Hz), the percentage frequency dependent susceptibility (χ_{FD}) was calculated. Important intrinsic variations were found for both M1 and M2 powders. Despite the variations, M2 powders exhibited statistically higher values (10% ± 7) compared to M1 powders (4% ± 3). The superparamagnetic content relates to the χ_{FD} values, indicating a relatively high superparamagnetic content for M2 samples (Dearing

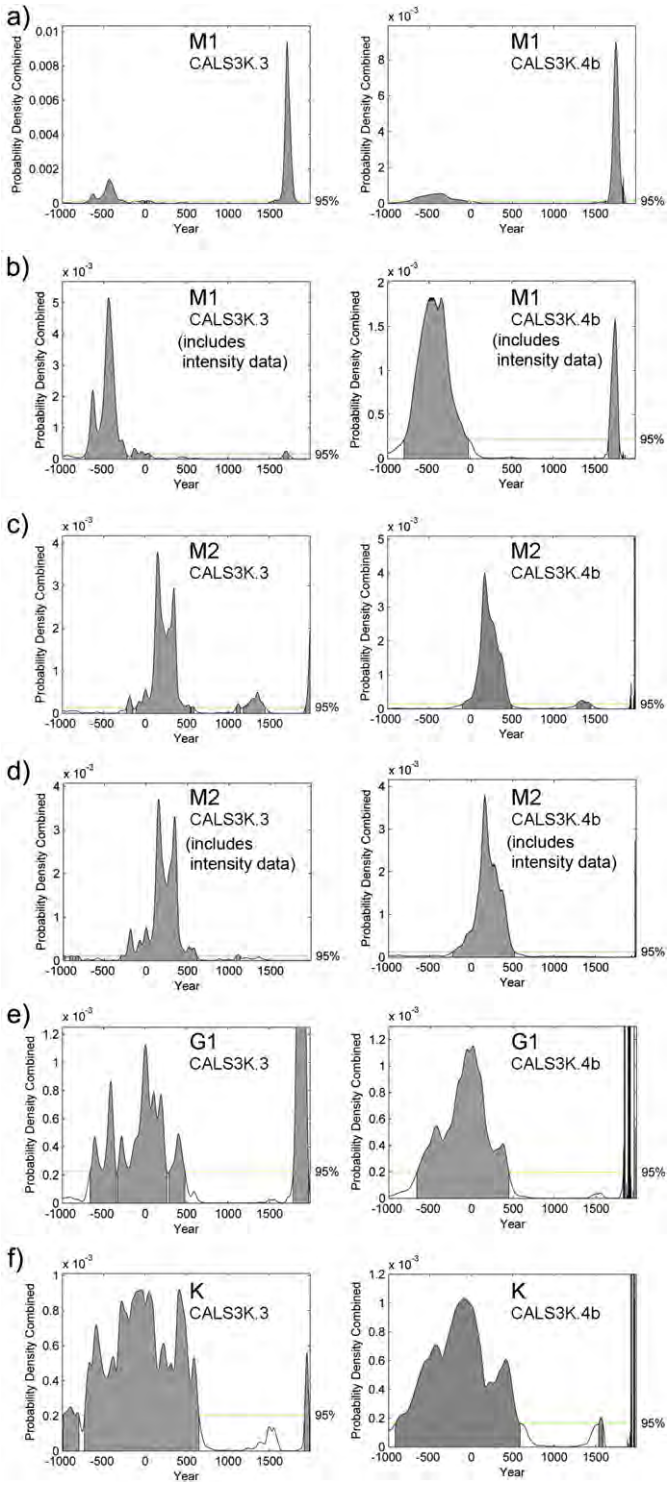

Fig. 9. Combined (declination and inclination (a), (c), (e) and (f), and also intensity (b) and (d)) probability functions obtained with the Matlab tool from Pavón-Carrasco et al. (2011) for the sampled kilns, using (left) CALS3K.3 and (right) CALS3K.4b models.

et al., 1996). Continuous susceptibility vs. temperature measurements revealed a relatively simple magnetic mineralogy for both M1 and M2 powders with high transition temperatures. For M1 powders, the susceptibility starts to decrease monotonously at around 400 °C, in contrast M2 powders exhibit a slight increase of susceptibility up to 450 °C (compatible with antiferromagnetic configurations) and then an abrupt decrease. Heating and cooling

Table 3
Archaeomagnetic ages using SCHA.DIF.3K, CALS3K.3 and CALS3K.4b geomagnetic models for kilns from El Maklouba (M1 and M2), El Gaala (G1) and Kerkouane (K = K1 + K2 + K3). Main solutions and maxima refer to the obtained probability time-distributions characterized by well-defined peaks if not otherwise specified. Presumed ages according to archaeological evidence are listed for comparison.

Kiln	Model	Main solutions	Maxima	Presumed archaeological age
M1	SCHA.DIF.3K	BC 417–144	340 BC	4th–1st BC or
		BC 96–17	62 BC	2nd–3rd AD
		AD 1687–1852	1754 AD	
	CALS3K.3	BC 690–255	434 BC	
		AD 1550–1831	1712 AD	
	CALS3K.4b	BC 747–45	354 BC	
		AD 1657–1836	1750 AD	
M2	SCHA.DIF.3K	AD 118–425	316 AD	
	CALS3K.3	BC 227–585	152 AD	
		AD 1099–1446	1355 AD	
		AD 1934–1990	1990 AD	
	CALS3K.4b	BC 97–AD 492	173 AD	
		AD 1969–1985	1979 AD	
G1	SCHA.DIF.3K	BC 68–AD 132	23 BC	Mid-4th BC–1st BC
		AD 170–268	219 AD	
		AD 377–483	429 AD	
		AD 1834–1900	1900 AD	
	CALS3K.3	BC 665–353	6 BC[a]	
		BC 335–AD 261	3 AD[a]	
		AD 289–479	399 AD	
		AD 1786–1973	1873 AD	
	CALS3K.4b	BC 669–AD 449	9 AD	
		AD 1840–1900	Highly spiky	
K	SCHA.DIF.3K	BC 60–AD 276	53 AD	Late-4th BC–3rd BC
		AD 352–490	428 AD	
		AD 1894–1990	1900 AD	
	CALS3K.3	BC 733–AD 649	44 BC, 408 AD[a]	
		AD 1923–1982	1952 AD	
	CALS3K.4b	BC 917–AD 587	73 BC	
		AD 1925–1972	1938 AD	

[a] Multipeak distributions.

paths are reasonably reversible for both kinds of powders (Fig. 10), indicating relatively high thermomagnetic stability and, therefore, that the samples can be used for Thellier-type archaeointensity determinations. Powdered slag fragments exhibited very low magnetic susceptibilities (specific mass susceptibility $<2\cdot10^{-8}$ m^3/kg). Their corresponding Mössbauer spectra show differences between grayish M1 and yellow/greenish M2 powders. The wider doublet signal of M1 indicates Fe^{2+} whereas that of M2 indicates

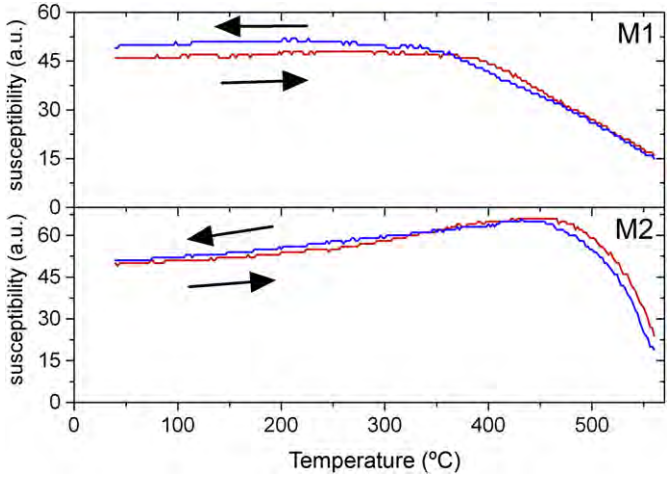

Fig. 10. Representative continuous susceptibility versus temperature curves for M1 and M2 powders. Maximum applied temperature was 560 °C. Arrows indicate the heating and cooling paths.

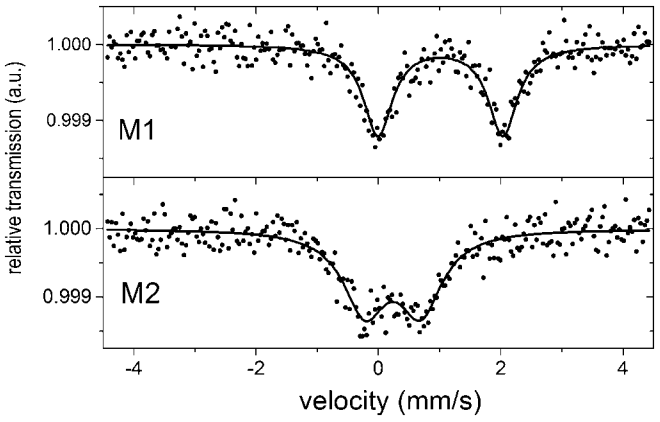

Fig. 11. Representative Mössbauer spectra for (top) M1 showing a Fe^{2+} paramagnetic doublet and (bottom) M2 showing a Fe^{3+} paramagnetic doublet.

Table 4
Archaeomagnetic intensity results from El Maklouba.

Specimen	*N*	*f*	*g*	*q*	*F* (μT)	F_{CR} (μT)	σ (μT)
M1i-1	7	0.82	0.78	11.03	59.29	–	5.37
M1i-2	7	0.93	0.75	25.75	77.26	72.37	3.00
M1i-3	7	0.55	0.81	6.07	40.74	35.72	6.71
M1i-4	7	0.91	0.76	15.15	76.32	72.40	5.04
M1i-5	6	0.59	0.78	27.57	64.89	–	2.35
M1i-6	7	0.90	0.78	14.92	78.10	75.19	5.23
M1i-7	6	0.79	0.67	10.53	75.44	74.69	7.17
M2i-1	5	0.87	0.38	9.05	64.55	–	7.13
M2i-2	5	0.86	0.64	62.33	68.39	64.04	1.10
M2i-4	6	0.85	0.57	21.7	64.34	57.92	2.97
M2i-5	7	0.84	0.64	18.07	61.34	56.70	3.40
Mi-1	6	0.75	0.75	11.84	64.29	59.19	5.43
Mi-2	7	0.56	0.81	9.99	57.41	–	5.75

Columns from left to right: Specimen, label of the specimen identifying the kiln provenance (M1, M2 or M); *N*, number of heating steps used for the intensity determination; *f*, fraction of NRM used for intensity determination; *g*, gap factor and *q*, quality factor as defined by Coe (1967); *F*, raw intensity; F_{CR}, cooling rate corrected intensity; σ, standard deviation of the intensity estimate.

Fe^{3+} (Fig. 11). This reveals different oxidation environments for M1 and M2 kilns. To sum up, Ti-poor titanomagnetite is probaly the magnetic carrier of M1 samples, whereas in M2 this role could be played by hemo-ilmenite.

Representative Arai plots of specimens from kilns M1 and M2 are shown in Fig. 12. A total of 16 specimens were analyzed (seven from kiln M1, seven from kiln M2 and two specimens from unidentified kilns), all of them exhibit linear Arai and Zijderveld plots. From these, only three were rejected (all of them from M2) due to negative pTRM checks, that is with a difference between the original pTRM and the pTRM check higher than 10 percent of the total TRM acquired (Chauvin et al., 2000). Angle deviation between the applied field direction and the acquired TRM was always below 7°. Cooling rate correction was applied to all specimens except five (three from M1, one from M2 and another from M) due changes in TRM acquisition capacity higher than 5%. Cooling rate correction factors always resulted in decreased archaeointensities ranging from 1% to 12%.

Table 4 lists the archaeointensity results for all the specimens that passed the pTRM checks and Fig. 13 shows plots of the sum of the corresponding individual archaeointensity results for M1 and M2 kilns. The sum of results from kiln M1 has been fitted to two Gaussians: a main peak centered at 70.68 μT and a secondary peak at only 35.80 μT, this secondary peak is due to a single specimen (M1i-3) that produced the lowest quality factor. This anomalous specimen was thus excluded from the computation of the representative intensity for kilns M1 (70.68 ± 7.92 μT). Concerning M2 kiln, despite the fact that the sum of results is actually bimodal, we have fitted it to a single Gaussian because the difference between the two modes is only around 6 μT. The single fitted Gaussian gives an archaeointensity estimate of 60.36 ± 5.26 μT. Results from the

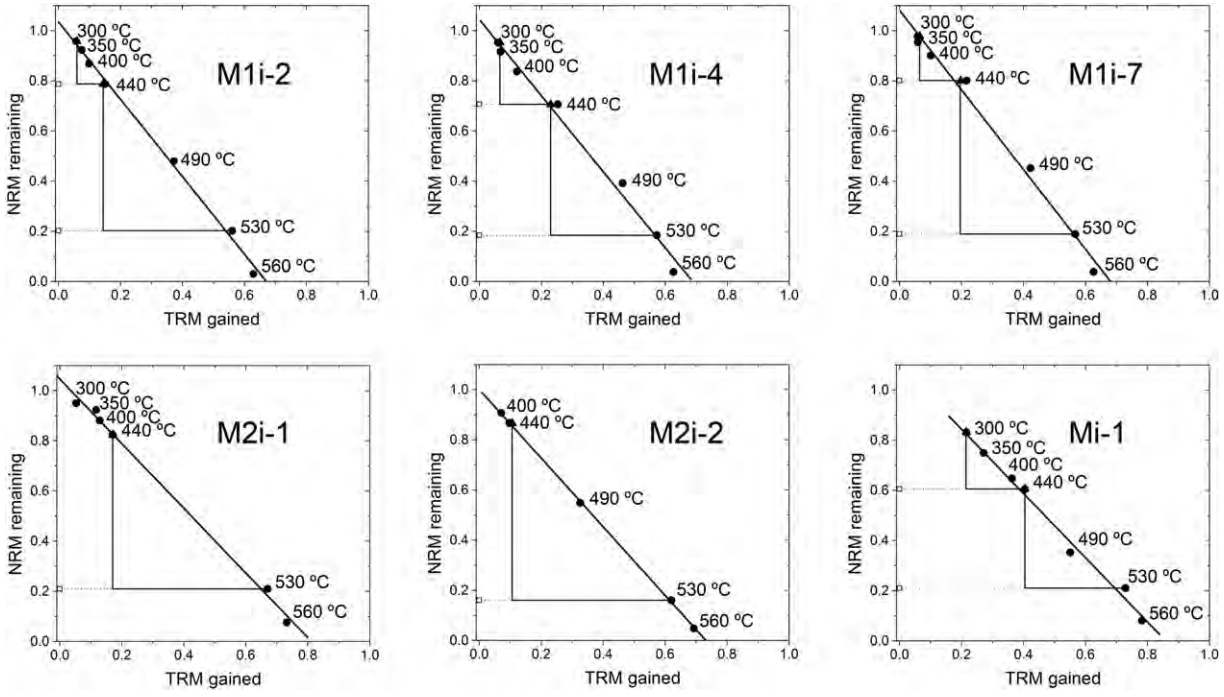

Fig. 12. Representative plots of normalized NRM remaining against TRM gained for specimens from El Maklouba kilns: (top) M1, (bottom) M2 and (bottom-right) unidentified.

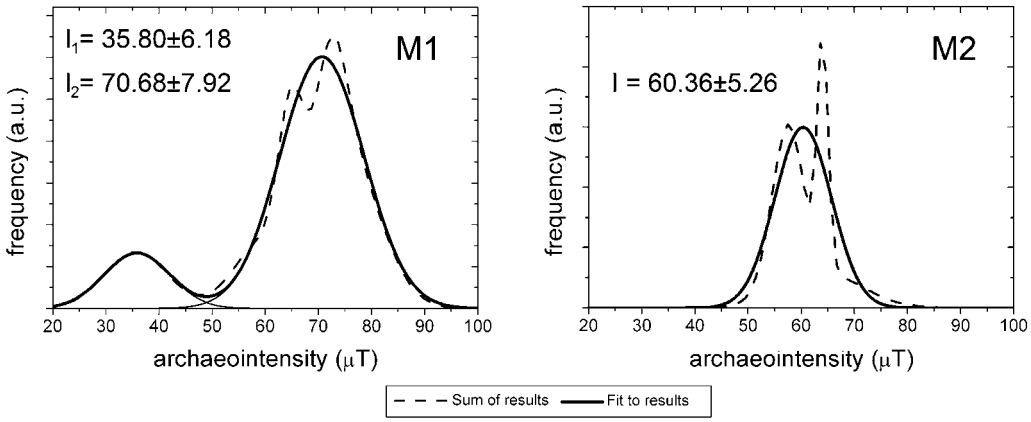

Fig. 13. Computation of mean archaeointensities for kilns from El Maklouba: (left) M1 and (right) M2. Dashed line is the sum of all accepted individual archaeointensity results for the kiln and solid line is the fitting to those sums.

two specimens of unidentified kilns produced 59.19 and 57.41 μT, thus close to the values obtained for kiln M2.

The obtained archaeointensity results were added to the experimental archaeodirections and compared with the SCHA.DIF.3K model obtaining a new probability distribution function with the most probable dates (see Fig. 7). One of the consequences of adding the intensity to the computation is the narrowing of the probable dates indicated by the distribution function, including the disappearance of the probability peak indicating ages within the 17th to 19th centuries. For the M1 kiln the new combined probability function indicates basically a single solution (BC 418–153). For the M2 kiln, the former time interval appears now divided in two (AD 102–185 and AD 243–422). It is worth to mention that the presented archaeointensities are not of very high quality because the number of single measurements is rather low and it is difficult to define the representative intensity value and its uncertainty. Besides this, the SCHA.DIF.3K model possibly does not still describe very accurately the evolution of the archaeointensity in the area under study. Despite these two drawbacks it is interesting to note that the mentioned effects of adding the intensity are almost invariably observed using the two tested CALS3K models (see Fig. 9b and d). This is a surprising result that points to an applicability of the archaeointensity measurements higher than expected from previous results (Fouzai et al., 2012) in the area under study and confirms the existing difference in the archaeomagnetic signature of the kilns M1 and M2. It is worth to note that no cooling rate correction was applied by Fouzai et al. (2012).

6. Conclusions

New archaeomagnetic data have been reported for Tunisia (four new archaeomagnetic directions and two new archaeomagnetic intensities). From these, data from Kerkuane can be associated to a well-known archaeological age (late-4th BC–3rd BC), whereas data from the other three sites would need a more constrained age determined from archaeological or non-magnetic archaeometric methods.

Far from being perfect, the SCHA.DIF.3K archaeomagnetic model indicates:

i) The last use of kiln M1 would have occurred within the BC 418–153 time interval, which is consistent with the first period of activity in the El Maklouba site as revealed by archaeological evidence (4th–1st century BC).
ii) The last use of kiln M2 would have occurred within the AD 102–422 time interval, which is consistent with the second period of activity in the El Maklouba site as revealed by archaeological evidence (2nd–3rd century AD).
iii) The last use of kiln G1 could have occurred within the BC 68–AD 136 time interval (maximum probability indicating year 24 BC), which is consistent with the archaeological hypothesis that associates the kiln with the Punic necropolis of El Gaala site, which was in use until the 1st century BC.

In contrast, neither SCHA.DIF.3K nor any of the tested CALS3K models produce solutions with time intervals within the known archaeological age of Kerkuane. We can outline three possible reasons: i) the models are not at all proficient (which is apparently inconsistent with the obtained good results for the neighboring sites of El Maklouba and El Gaala), ii) a remagnetization of the structures of the site occurred later than the occupation of the site (such remagnetization should have produced archaeological evidences not reported) and iii) the limited number of collected data in Kerkuane and its hybrid nature (samples were gathered from three different kilns are analyzed together) produces the observed disagreement. We opt for the latter, and future work will include resampling at Kerkuane to increase the number of measurements. Data treatment should be done individually for each kiln and should include intensity estimates. Given that Kerkuane is a touristic and exceptional site, and from the acquired experience, the best candidates to perform resampling are the lime kilns.

Archaeomagnetic dating techniques applied to two of the kilns from El Maklouba have permitted to associate them to the different chronological archaeological phases of a site that amounts at least 12 kilns. This should be taken into account if a systematic excavation in the site was ever performed. If the suggested chronology was confirmed by non-magnetic methods, the archaeointensity distinction between the two periods (4th–1st century BC and 2nd–3rd century AD) would suggest that the high geomagnetic intensity recorded in eastern Europe (Pavón-Carrasco et al., 2009) is also observed in Tunisia.

From a wider point of view, the data presented here add to the recently published archaeomagnetic data from Tunisia increasing the knowledge of the local geomagnetic field and emphasizing the potential of Tunisia as a target country to carry out archaeomagnetic studies. This kind of studies should be encouraged and considered as a possible dating resource for archaeologists interested in northern Africa. Combined archaeodirection and archaeointensity studies similar to the one undertaken in El Maklouba

should be extended, when possible, to other Tunisian and North African sites.

Acknowledgments

We are grateful to Nejib Ben Lazreg and Habib Ben Younés from the Institut National du Patrimoine for authorizing sampling on the studied sites. Jihene Nacef from the Institut Supérieur des Études Appliquées en Humanités de Mahdia is also acknowledged for its support to access some of the sites. We thank Siwar Baklouti and Marta Moreno for their support during field work. We also would like to acknowledge two anonymous reviewers for their helpful and insightful comments. This research is part of the collaboration between the Unité de Recherche Pétrologie cristalline et sédimentaire de l'Université Tunis El Manar and the Geology Department (Universitat Autònoma de Barcelona) through funds by the Spanish Ministerio de Ciencia e Innovación (project HAR2010-16953) and the Agencia Española de Cooperación Internacional para el Desarrollo (Spain-Tunisia bilateral project A1/039844/11).

References

Ben Lazreg, N., Duval, N., 1995. Le baptistère de Bekalta. In: Paris-Musées (Ed.), Carthage, l'histoire, sa trace et son écho. Paris-Musées, Paris, pp. 304–306.

Ben Younés, H., 2002. El Gaala site périphérique de la Ville de Thapsus (Ras Dimas) à l'époque préromaine. Note préliminaire. In: Africa, Serie Reppal, vol. XII. Institut National du Patrimoine, pp. 9–15.

Carvallo, C., Roberts, A.P., Leonhardt, R., Laj, C., Kissel, C., Perrin, M., Camps, P., 2006. Increasing the efficiency of paleointensity analyses by selection of samples using first-order reversal curve diagrams. Journal of Geophysical Research 111, B12103. http://dx.doi.org/10.1029/2005JB004126.

Casas, L.L., Incoronato, A., 2007. Distribution analysis of errors due to relocation of geomagnetic data using the 'Conversion via Pole' (CVP) method: implications on archaeomagnetic data. Geophysical Journal International 169, 448–454.

Casas, L.L., Briansó, J.L., Álvarez, A., Benzzi, K., Shaw, J., 2008. Archaeomagnetic intensity data from the Saadien Tombs (Marrakech, Morocco), late 16th century. Physics and Chemistry of the Earth 33, 474–480. Parts A/B/C.

Chauvin, A., Garcia, Y., Lanos, P., Laubenheimer, F., 2000. Paleointensity of the geomagnetic field recovered on archaeomagnetic sites from France. Physics of the Earth and Planetary Interiors 120, 111–136.

Coe, R.S., 1967. Paleo-intensities of Earth's magnetic field determined from tertiary and quaternary rocks. Journal of Geophysical Research 72, 3247–3262.

Dearing, J.A., Dann, R.J.L., Hay, K., Lees, J.A., Loveland, P.J., Maher, B.A., O'Grady, K., 1996. Frequency-dependent susceptibility measurements of environmental materials. Geophysical Journal International 124, 228–240.

Fantar, M.H., 1984. Kerkouane cité punique du Cap Bon (Tunisie), tome I. Institut National d'Archéologie et d'Art, Tunis.

Fantar, M.H., 1986. Kerkouane cité punique du Cap Bon (Tunisie), tome III. Institut National d'Archéologie et d'Art, Tunis.

Fantar, M.H., 2000. L'urbanisme et l'architecture puniques, le cas de Kerkouane, pp. 71–88.

Fisher, R., 1953. Dispersion on a Sphere. Proceedings of the Royal Society of London. Series A. Mathematical and Physical Sciences 217, 295–305.

Fouzai, B., Casas, Ll., Laridhi Ouazaa, N., Álvarez, A., 2012. Archaeomagnetic data from four Roman sites in Tunisia. Journal of Archaeological Science 39, 1871–1882.

Gibbins, D., 2001. A Roma shipwreck of c.AD200 at Plemmirio, Sicily: evidence for north African amphora production during the Severan period. World Archaeology 32, 311–334.

Gomez-Paccard, M., McIntosh, G., Chauvin, A., Beamud, E., Pavon-Carrasco, F.J., Thiriot, J., 2012. Archaeomagnetic and rock magnetic study of six kilns from North Africa (Tunisia and Morocco). Geophysical Journal International 189, 169–186.

Kirschvink, J.L., 1980. The least-squares line and plane and the analysis of paleomagnetic data. Geophysical Journal of the Royal Astronomical Society 62, 699–718.

Korte, M., Donadini, F., Constable, C.G., 2009. Geomagnetic field for 0–3 ka: 2. A new series of time-varying global models. Geochemistry, Geophysics, Geosystems 10, Q06008.

Korte, M., Constable, C., 2011. Improving geomagnetic field reconstructions for 0–3 ka. Physics of the Earth and Planetary Interiors 188, 247–259.

Kovacheva, M.A., 1984. Some Archaeomagnetic Conclusions from 3 Archaeological Localities in Northwest Africa, vol. 37. Dokladi Na Bolgarskata Akademiya Na Naukite. 171–174.

Kovacheva, M., Chauvin, A., Jordanova, N., Lanos, Ph., Karloukovski, V., 2009. Remanence anisotropy effect on the palaeointensity results obtained from various archaeological materials, excluding pottery. Earth Planets Space 61, 711–732.

Morel, J., 1969. Kerkouane, ville punique du cap Bon: remarques archéologiques et historiques. Mélanges d'archéologie et d'histoire 81, 473–518.

Najid, D., 1986. Palaeomagnetic studies in Morocco, PhD thesis, University of Newcastle upon Tyne.

Pasa, B., 2011. Recherches sur l'Africa vetus, de la destruction de Carthage aux interventions césaro-augustéennes, PhD thesis, Université de Toulouse.

Pavón-Carrasco, F.J., Osete, M.L., Torta, M., Gaya-Piqué, L.R., 2009. A regional archeomagnetic model for Europe for the last 3000 years, SCHA.DIF.3K: applications to archeomagnetic dating. Geochemistry Geophysics Geosystems 10, Q03013.

Pavón-Carrasco, F.J., Rodríguez-González, J., Osete, M.L., Torta, M., 2011. A Matlab tool for archaeomagnetic dating. Journal of Archaeological Science 38, 408–419.

Peacock, D.P.S., Bejaoui, F., Belazreg, N., 1989. Roman Amphora Production in the Sahel Region of Tunisia, vol. 114. Publications de l'École française de Rome. 179–222.

Taylor, R.J., Robinson, V.J., Gibbins, D.J.L., 1997. An investigation of the provenance of the Roman amphora cargo from the Plemmirio B shipwreck. Archaeometry 39, 9–21.

Thellier, E., Thellier, O., 1959. Sur l'intensité du champ magnétique terrestre dans le passé historique et géologique. Annales de Géophysique 15, 285–376.